CFD Letters

Journal homepage:
https://semarakilmu.com.my/journals/index.php/CFD_Letters/index
ISSN: 2180-1363

# Numerical Investigation of $Ti_3C_2$ MXene Nanofluid Convective Heat Transfer Performance in Circular Tube

Ridho Irwansyah[1,*], Dieter Rahmadiawan[2,3], Dedison Gasni[4], Kevin Raynaldo[5]

[1] Laboratory of Fluid Mechanics, Department of Mechanical Engineering, Faculty of Engineering, Universitas Indonesia, Depok 16424, West Java, Indonesia
[2] Department of Mechanical Engineering, National Cheng Kung University (NCKU), Tainan, Taiwan
[3] Department of Mechanical Engineering, Universitas Negeri Padang, 25173 Padang, Sumatera Barat, Indonesia
[4] Department of Mechanical Engineering, Faculty of Engineering andalas University, Kampus Limau Manis, Padang 25163, Indonesia
[5] Study Program of Mechanical Engineering, Faculty of Engineering, Universitas Tarumanagara, Jl. Letjen S. Parman No. 1, Jakarta 11440, Indonesia

**ARTICLE INFO**

***Article history:***
Received 8 August 2024
Received in revised form 12 September 2024
Accepted 17 December 2024
Available online 31 January 2025

***Keywords:***
$Ti_3C_2$ nanofluid; multi-objective optimization; nanofluid effective properties

**ABSTRACT**

$Ti_3C_2$ Mxene exhibits promising thermophysical properties and heat transfer performance, rendering it a potentially valuable material for industrial applications. In the present study, water and water-CMC (Carboxymetthyl Cellulose) are selected as the base fluids. However, the lack of research on characterization and heat transfer performance studies encourages the present research. Subsequently, Computational Fluid Dynamics (CFD) is employed to analyse the heat transfer performance and pressure drop of each variable utilising the effective properties method for single-phase nanofluids. Given that an increase in nanofluid heat transfer tends to result in an elevated pressure drop, Design Expert optimization is employed to analyse multi-objective optimization. This study aims to optimize the heat transfer of $Ti_3C_2$ nanofluid. This research uses a Circular tube as a test section and acts as a fluid domain. Based on the CFD simulation, water-CMC can significantly increase the average Nusselt number with better heat transfer performance. The pressure drop of water-CMC is also gradually increasing. Based on Design Expert numerical optimization, the most optimum $Ti_3C_2$ nanofluid satisfied increasing heat transfer performance and decreasing pressure drop is $Ti_3C_2$-Water-CMC 0.35wt% (0.083vol%) nanofluid. This nanofluid has 74.514 for the Nusselt number and 1998.739 Pa for the pressure drop.

## 1. Introduction

Three decades after the idea of using suspended nanometre-sized solid particles in base fluids was first proposed by Choi *et al.,* [1], nanofluids have gained the attention of numerous researchers to provide a solution for better heat transfer performance. Nanofluids typically comprise metal, metal oxides or carbon nanomaterials dispersed in the base fluids. Studies have been focused on the effective thermal properties [2,3] and heat transfer performance of nanofluids [4,5]. Several

* *Corresponding author.*
*E-mail address: ridho.irwansyah04@ui.ac.id (Ridho Irwansyah)*

https://doi.org/10.37934/cfdl.17.7.130141

parameters, such as volume concentration, particle size and particle shape, have been identified as the source of nanofluids' enhanced heat transfer performance [6,7].

Recently, a new type of nanoparticle was discovered. It has a unique two-dimensional structure with a layered-like structure. The newly developed nanoparticle is called MXene [8] and it offers distinctive electrical, optical and mechanical capabilities due to the adaptability of its structural flexibility and surface features [9]. These traits make them promising for various applications in sensors, catalysis, biomedicine, energy storage and ion batteries [10]. MXene nanomaterials have eco-friendly characteristics and promising thermophysical properties [11]. The addition of MXene nanoparticles in silicone oil improved the electrical efficiency of the photovoltaic (PV) module due to its cooling performance [12]. The application of MXene nanofluid for photovoltaic cooling system was explored by Samylingam *et al.,* [13], showing an overall efficiency improvement.

Moreover, Mao *et al.,* utilized the MXene-based ($Ti_3C_2T_x$) nanofluid and found an increase in thermal conductivity with a slight increase in dynamic viscosity, thus promising to be implemented as an industrial coolant [9]. $Ti_3C_2$ is a widely used MXene nanoparticle due to its better heat transfer performance. Furthermore, combining water and CMC (Carboxymethyl Cellulose) additives provides promising stability and heat transfer performance [14]. Nevertheless, $Ti_3C_2$ nanofluid is still relatively new, so there is a lack of research focused on characterization and heat transfer performance study of it. Therefore, this research analyses the heat transfer performance of $Ti_3C_2$ nanofluid.

Nanofluids heat transfer can be simulated through two different approaches. The first approach uses a multiphase model where the base fluid and nanoparticles are simulated in a separate phase with their respective properties. Furthermore, several studies have shown that nanofluids can also be simulated as a single phase by taking into account the effective properties of the mixture. A report by Minea *et al.,* [15] provided a comparison of the two approaches. Dehghan *et al.,* [16] for instance, numerically investigated the heat transfer performance of graphene oxide/water nanofluids over a double backward-facing microchannel using the effective properties of the mixture. Elfaghi *et al.,* [17] numerically investigated heat transfer enhancement with the use of $Al_2O_3$/water nanofluid utilizing single phase model.

The objective of this study is to numerically investigate the laminar convective heat transfer of $Ti_3C_2$ nanofluids in a circular tube is numerically investigated. Based on the previous study, the heat transfer performance of the nanofluids and the pressure drop will be carefully analysed. Further analysis using multi-objective optimization will be performed to determine the optimum heat transfer enhancement with a minimum increase in pressure drop.

## 2. Methodology

### *2.1 Material*

The initial work in this study was performed by examining the convective heat transfer of water. The initial result will be used as a baseline for comparison and to validate the results with existing literature. Furthermore, four different nanofluids, a combination of $Ti_3C_2$-Water 0.35wt%, $Ti_3C_2$-Water-CMC 0.35wt%, $Ti_3C_2$-Water 0.7wt% and $Ti_3C_2$-Water-CMC 0.7wt% will also be simulated. The thermal properties of nanofluids were adapted from Rahmadiawan *et al.,* [14] and are listed in Table 1. The density and the heat capacity of nanofluids are calculated using Eq. (6) and Eq. (7), respectively.

**Table 1**
Thermophysical properties of working fluids [14]

| Thermo-physical Properties | Fluid (at 30 °C) | | | | |
|---|---|---|---|---|---|
| | Water | $Ti_3C_2$-Water 0.35wt% (0.083 vol%) | $Ti_3C_2$-Water-CMC 0.35wt% (0.083 vol%) | $Ti_3C_2$-Water 0.7wt% (0.166 vol%) | $Ti_3C_2$-Water-CMC 0.7wt% (0.166 vol%) |
| Dynamic Viscosity (Pa s) | 0.001006 | 0.001052 | 0.003409 | 0.001458 | 0.003654 |
| Thermal Conductivity (W/mK) | 0.6000 | 0.7272 | 0.7613 | 0.8403 | 0.9129 |

## *2.2 Test Section*

The present study uses a circular tube with 8 mm of diameter and 2000 mm length, identical to Minea *et al.,* [15]. Figure 1 shows the geometry with 10 points where the temperature data will be collected.

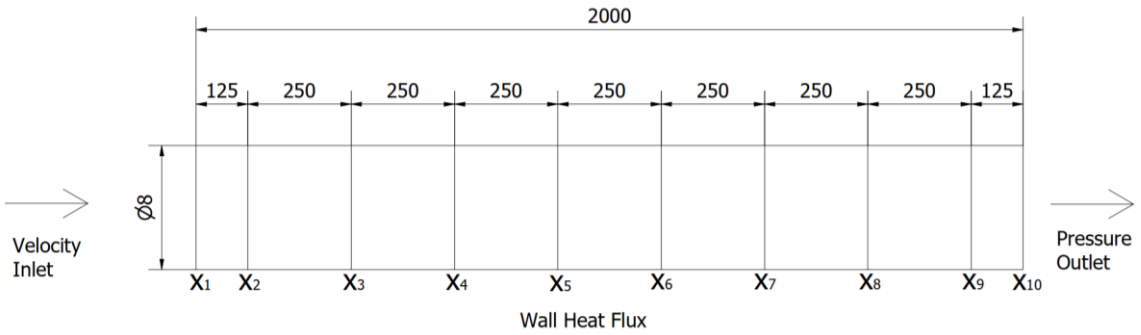


**Fig. 1.** Schematic of the test section (unit in mm)

## *2.3 Numerical Model*

In this study, the governing equations are solved by the Ansys Fluent. Furthermore, to validate the geometry, a grid-independent study is performed. Three different mesh configurations were used, which were 764,235 (coarse); 2,562,435 (fine); and 5,359,635 (finer). The meshing process was performed using Ansys ICEM, as shown in Figure 2. The results were processed and plotted as a function between the Nusselt number and the number of cells.

**Fig. 2.** Mesh configuration for current research

Furthermore, Figure 3 shows that the fine and finer meshes showed only a 3% deviation. Thus, further simulations will be performed using the fine mesh configuration.

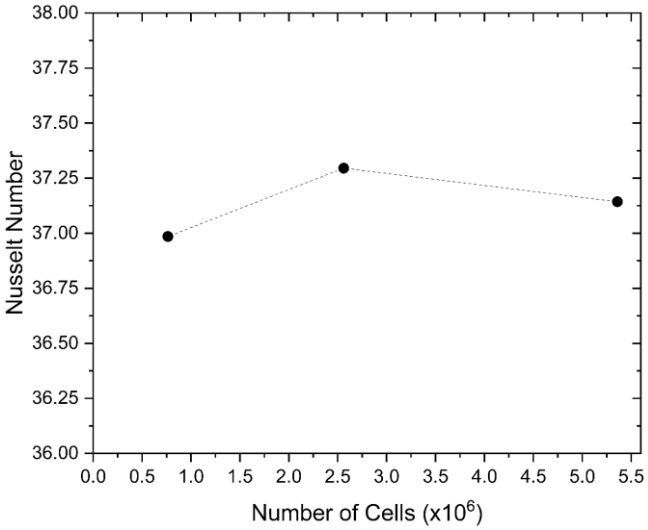


**Fig. 3.** Mesh independency study for current research

A preliminary study was conducted to validate the heat transfer. Two sets of working fluids, water and $TiO_2$-water 2%, were simulated at a constant heat of 100 Watt and inlet flow rate of 6 g/s. The present results were further compared to that of Minea *et al.,* [15]. A comparison between the present result and the literature for pure water can be seen in Figure 4 and the 2.5% $TiO_2$-water nanofluid can be seen in Figure 5. An average error for each comparison of the present research to the literature is less than 5%. Thus, the numerical setup can be used further.

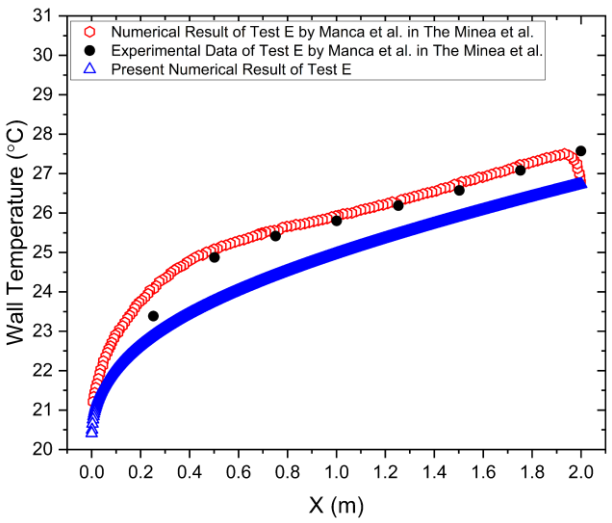


**Fig. 4.** Comparison of pure-water flow with 6 g/s and 100-Watt heat

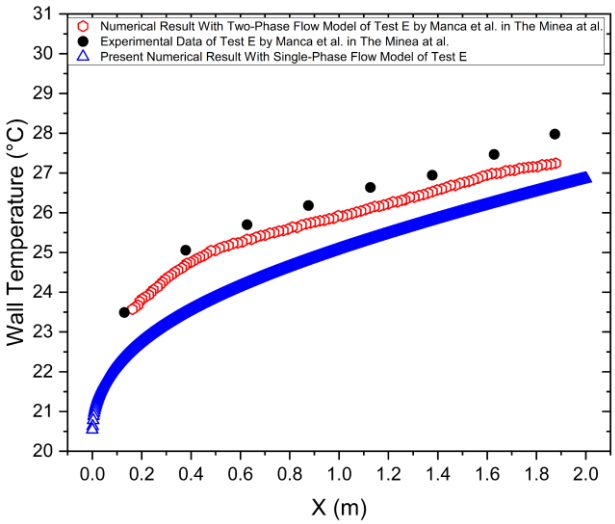


**Fig. 5.** Comparison of 2.5% TiO2-water nanofluid flow with 6 g/s and 100-Watt heat

### *2.4 Research Design*

This research has factors and levels, as tabulated in Table 2. A total of 40 combinations of boundary conditions were simulated with an identical inlet temperature of 25 $^0$C. Moreover, the output of the present research is the average Nusselt number and pressure drop.

**Table 2**
Research design

| No. | Factor | Level | | | | |
|---|---|---|---|---|---|---|
| 1 | Reynolds Number | 400 | 800 | 1200 | 1600 | |
| 2 | Wall Heat Flux (W/m$^2$) | 2000 | 4000 | | | |
| 3 | Working Fluid | Water | $Ti_3C_2$-Water 0.35wt% (0.083 vol%) | $Ti_3C_2$-Water-CMC 0.35wt% (0.083 vol%) | $Ti_3C_2$-Water 0.7wt% (0.166 vol%) | $Ti_3C_2$-Water-CMC 0.7wt% (0.166 vol%) |

### *2.5 Governing Equations*

The heat transfer performance and flow characteristic of $Ti_3C_2$ nanofluids in a circular tube is solved utilizing the equations of continuity, momentum and energy in the ANSYS Fluent and the equations are provided using some assumptions as follows:

i. The flow is laminar and three-dimensional.
ii. Effective thermophysical properties of the nanofluids are considered.
iii. The flow is steady state and single phase (effective thermophysical properties model).
iv. The nanofluid is incompressible and Newtonian.
v. There is no natural convection effect.

The following equations are written based on the assumption before in a cylindrical coordinates system, which is suitable for circular tubes:

Continuity equation [18]:

$$\frac{1}{r}\frac{\partial(rv_r)}{\partial r}+\frac{1}{r}\frac{\partial(v_\theta)}{\partial \theta}+\frac{\partial(v_z)}{\partial z}=0 \tag{1}$$

Momentum equation for r-axis [18]:

$$\rho_{nf}\left(v_r\frac{\partial v_r}{\partial r}+\frac{v_\theta}{r}\frac{\partial v_r}{\partial \theta}-\frac{{v_\theta}^2}{r}+v_z\frac{\partial v_r}{\partial z}\right)=-\frac{\partial p}{\partial r}+\rho_{nf}g_r+\mu_{nf}\left[\frac{1}{r}\frac{\partial}{\partial r}\left(r\frac{\partial v_r}{\partial r}\right)-\frac{v_r}{r^2}+\frac{1}{r^2}\frac{\partial^2 v_r}{\partial \theta^2}-\frac{2}{r^2}\frac{\partial v_\theta}{\partial \theta}+\frac{\partial^2 v_r}{\partial z^2}\right] \tag{2}$$

Momentum equation for θ-axis [18]:

$$\rho_{nf}\left(v_r\frac{\partial v_\theta}{\partial r}+\frac{v_\theta}{r}\frac{\partial v_\theta}{\partial \theta}+\frac{v_r v_\theta}{r}+v_z\frac{\partial v_\theta}{\partial z}\right)=-\frac{1}{r}\frac{\partial p}{\partial \theta}+\rho_{nf}g_\theta+\mu_{nf}\left[\frac{1}{r}\frac{\partial}{\partial r}\left(r\frac{\partial v_\theta}{\partial r}\right)-\frac{v_\theta}{r^2}+\frac{1}{r^2}\frac{\partial^2 v_\theta}{\partial \theta^2}+\frac{2}{r^2}\frac{\partial v_r}{\partial \theta}+\frac{\partial^2 v_\theta}{\partial z^2}\right] \tag{3}$$

Momentum equation for z-axis [18]:

$$\rho_{nf}\left(v_r\frac{\partial v_z}{\partial r}+\frac{v_\theta}{r}\frac{\partial v_z}{\partial \theta}+v_z\frac{\partial v_z}{\partial z}\right)=-\frac{\partial p}{\partial z}+\rho_{nf}g_z+\mu_{nf}\left[\frac{1}{r}\frac{\partial}{\partial r}\left(r\frac{\partial v_z}{\partial r}\right)+\frac{1}{r^2}\frac{\partial^2 v_z}{\partial \theta^2}+\frac{\partial^2 v_z}{\partial z^2}\right] \tag{4}$$

Energy equation [19]:

$$\frac{1}{r}\frac{\partial}{\partial r}\left(r\rho_{nf}Cp_{nf}Tv_r\right)+\frac{1}{r}\frac{\partial}{\partial\theta}\left(\rho_{nf}Cp_{nf}Tv_\theta\right)+\frac{\partial\left(\rho_{nf}Cp_{nf}Tv_z\right)}{\partial z}=\frac{1}{r}\frac{\partial}{\partial r}\left(\frac{k_{nf}}{\rho_{nf}Cp_{nf}}\frac{\partial T}{\partial r}\right)+\frac{1}{r^2}\frac{\partial}{\partial\theta}\left(\frac{k_{nf}}{\rho_{nf}Cp_{nf}}\frac{\partial T}{\partial\theta}\right)+\frac{\partial}{\partial z}\left(\frac{k_{nf}}{\rho_{nf}Cp_{nf}}\frac{\partial T}{\partial z}\right)+\frac{\dot{q}}{\rho_{nf}} \quad (5)$$

Where: $r$ represents radius (m); $v_r$, $v_\vartheta$ *and* $v_z$ represent velocity respect to r-axis, θ-axis and z-axis, respectively (m/s); $\rho_{nf}$ represents density of nanofluid (kg/m$^3$); $p$ represents pressurre (Pa)*;* $g_r$, $g_\vartheta$ *and* $g_z$ represent gravity acceleration respect to r-axis, θ-axis and z-axis, respectively (m/s$^2$); $\mu_{nf}$ represents dynamic viscosity of nanofluid (Pa s); $Cp_{nf}$ represents specific heat of nanofluid (J/kg K); $T$ represents temperature (K); $k_{nf}$ represents thermal conductivity of nanofluid (W/mK); and $\dot{q}$ represents rate of heat generation per unit volume (W/m$^3$).

Furthermore, to find the effective thermophysical properties, some equations are used: effective density of nanofluid (Eq. (6)) [20] and effective specific heat of nanofluid (Eq. (7)) [21].

$$\rho_{nf}=\varphi\rho_s+(1-\varphi)\rho_f \quad (6)$$

$$\left(C_p\rho\right)_{nf}=\varphi\left(C_p\rho\right)_s+(1-\varphi)\left(C_p\rho\right)_f \quad (7)$$

Where: $\varphi$ represents volume fraction; $\rho_s$ and $\rho_f$ represent density of solid nanoparticle and base fluid, respectively (kg/m$^3$); $Cp_s$ and $Cp_f$ represent specific heat of solid nanoparticle and base fluid, respectively (J/kg K).

The volume and mass fraction relationship of the nanoparticle in the solution can be calculated using Eq. (8) [11]. Moreover, the local convective heat transfer coefficient and average Nusselt number can be calculated using Eq. (9) and Eq. (10), respectively [11].

$$\varphi=\frac{\psi\rho_f}{\rho_s+\psi\rho_f-\psi\rho_s} \quad (8)$$

$$h_{local}=\frac{q"}{T_{wall}-T_{bulk}} \quad (9)$$

$$Nu_{avg}=\frac{h_{avg}D_h}{k_{nf}} \quad (10)$$

Where: $\psi$ represents mass fraction; $h_{local}$ represents convective heat transfer coefficient at which analysis conducted at the specific certain cross-section (W/m$^2$k); $q"$ represents wall heat flux (W/m$^2$); $D_h$ represents hydraulic diameter (m); $T_{wall}$ and $T_{bulk}$ represent temperature at which analysis conducted at the wall and conducted at the mean value of fluid flow, respectively (K); $Nu_{avg}$ represents Nusselt number average; $h_{avg}$ represents convective heat transfer coefficient average (W/m$^2$k).

## 3. Results

### *3.1 Heat Transfer Performance*

In this study, the constant wall heat flux approach was employed, resulting in a gradual increase in fluid temperature as it flows from the inlet to the outlet. The temperature contour of $Ti_3C_2$-Water-

CMC 0.35wt% at Reynolds number of 1600 and heat flux of 2000 and 4000 W/m$^2$ are depicted in Figure 6(a) and 6(b), respectively.

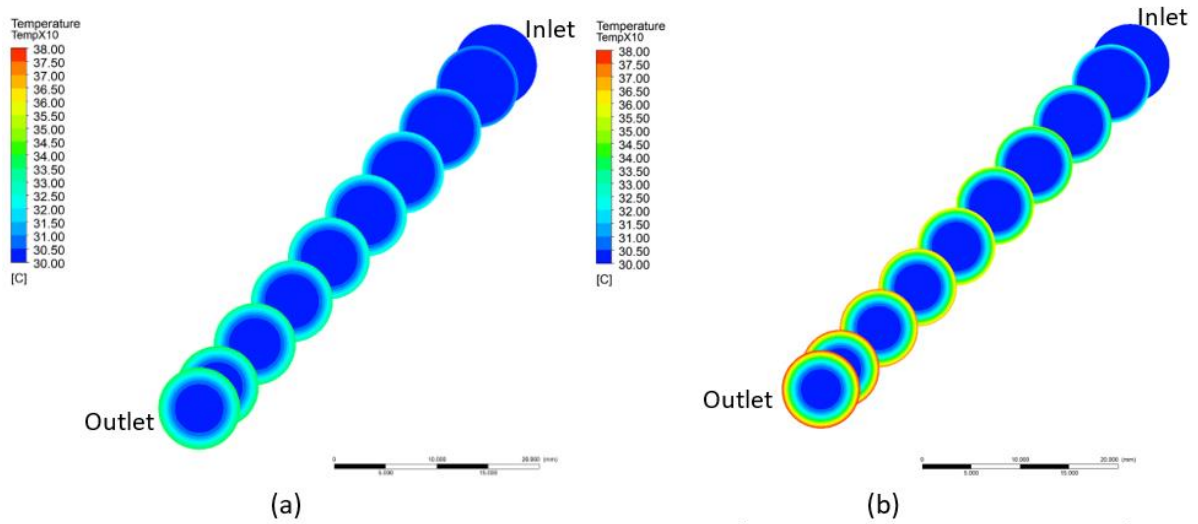


**Fig. 6.** Temperature contour for: (a) Run 18 for q" = 2000 W/m$^2$ (b) Run 38 for q" = 4000 W/m$^2$

Moreover, Figure 7(a) and 7(b) show the bulk outlet temperature as a function of Reynolds number under the variation of working fluids. The results show that the temperature decreases as the Reynolds number increases and the $Ti_3C_2$-Water-CMC 0.7wt% has the lowest temperature compared to other working fluids.

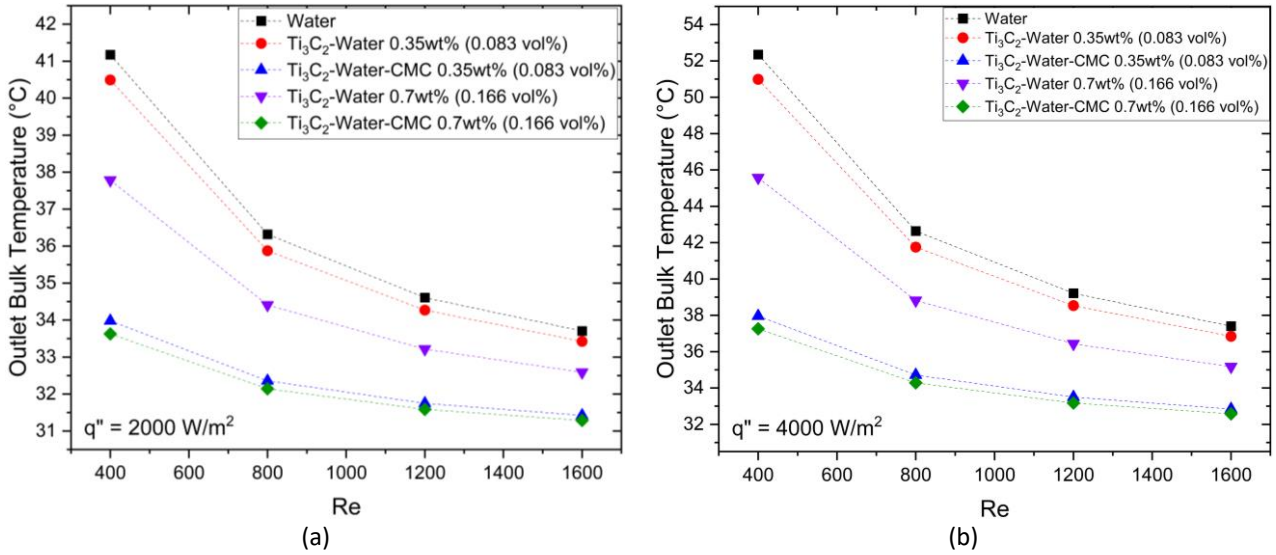


**Fig. 7.** Outlet bulk temperature variation with Reynolds number for (a) q" = 2000 W/m$^2$ (b) q" = 4000 W/m$^2$

The addition of nanoparticles to the base fluid will increase the convective heat transfer coefficient for the same Reynolds number. Thus, increasing the Reynolds number with the same nanofluids will also increase the convective heat transfer coefficient as depicted in Figure 8. The highest heat transfer coefficient was achieved by $Ti_3C_2$-Water-CMC 0.7wt% nanofluids and other nanofluids show a higher heat transfer coefficient than water. $Ti_3C_2$-Water-CMC 0.7wt% (0.166vol%) shows the highest increase in average convective heat transfer coefficient of 108.81% compared to that of water at Reynolds numbers of 1600 and 2000 W/m$^2$ of wall heat flux. Furthermore, $Ti_3C_2$-

Water-CMC 0.7wt% (0.166vol%) also has a convective heat transfer enhancement of 108.82% compared to that of Water at Reynolds numbers of 1600 and 4000 W/m$^2$ of wall heat flux.

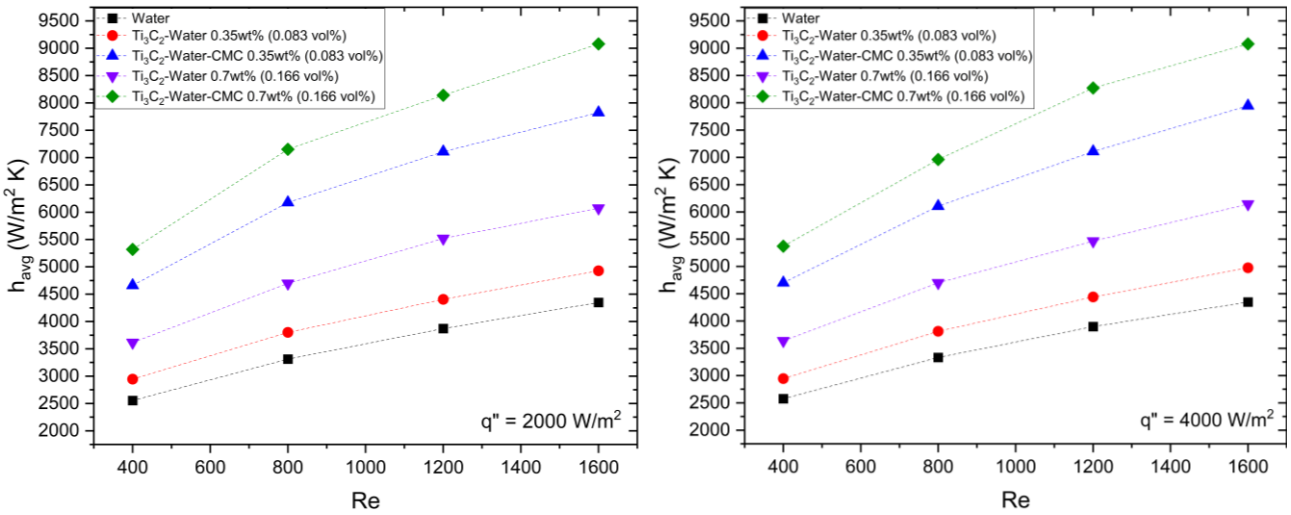


(a) (b)

**Fig. 8.** Average convective heat transfer coefficient ($h_{avg}$) variation with Reynolds number for: (a) q" = 2000 W/m$^2$ (b) q" = 4000 W/m$^2$

Furthermore, a non-dimensional Nusselt number will be used to assess the heat transfer performance of $Ti_3C_2$ nanofluid further. Figure 9 shows that the Nusselt number of $Ti_3C_2$-Water 0.35wt% nanofluid is lower than water. Then, the Nusselt number of $Ti_3C_2$-Water 0.7wt% nanofluid is slightly increased against water. These phenomena imply that the increase of convective heat transfer coefficient (*h*) is not significant against the increase of thermal conductivity. Furthermore, the increase of the Nusselt number of $Ti_3C_2$-Water-CMC 0.35wt% nanofluid is higher than the increase of the Nusselt number of $Ti_3C_2$-Water-CMC 0.7wt% nanofluid, which also means the increase of convective heat transfer coefficient is not significant compared to the increase of the thermal conductivity. However, adding nanoparticles increases the pressure drop as seen in Figure 10. The presence of CMC in the base fluid also contributed to raising the pressure drop.

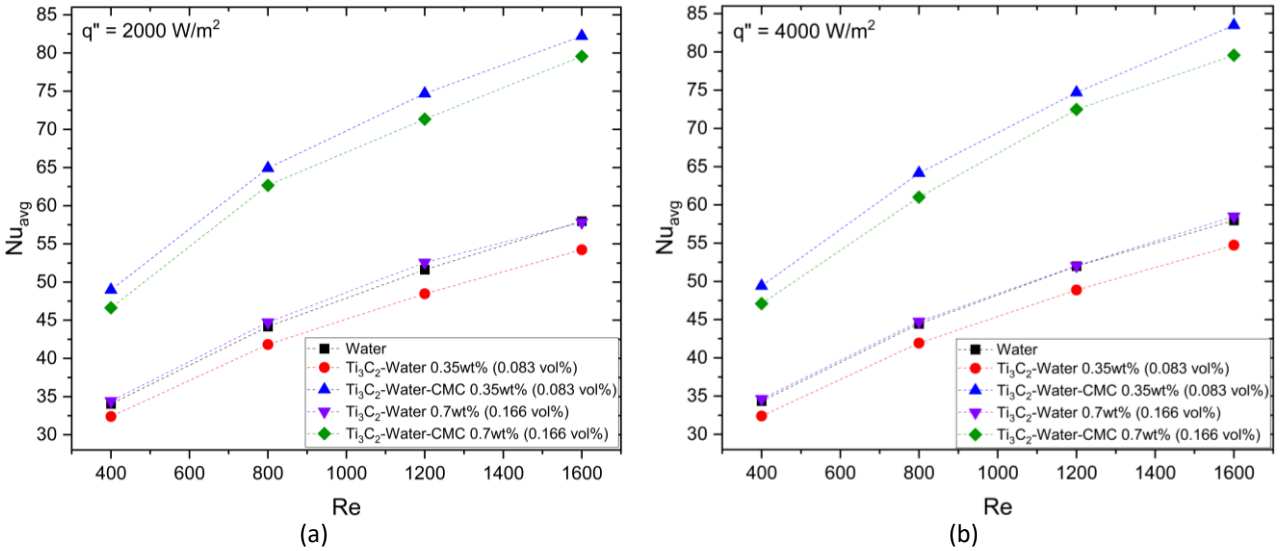


(a) (b)

**Fig. 9.** Average Nusselt number ($Nu_{avg}$) variation with Reynolds number for: (a) q" = 2000 W/m$^2$ (b) q" = 4000 W/m$^2$

$Ti_3C_2$-Water-CMC 0.35wt% (0.083vol%) has the highest average Nusselt number enhancement of 41.822% at Reynolds numbers of 1600 and 2000 W/m$^2$ of wall heat flux. Moreover, $Ti_3C_2$-Water-CMC 0.35wt% (0.083vol%) has 44.015% Nusselt number enhancement at Reynolds numbers of 1600 and 4000 W/m$^2$ of wall heat flux. These results imply that the average convective heat transfer coefficient enhancement is not significant compared to the enhancement of nanofluids thermal conductivity, which is obtained from nanoparticle addition to the base fluid. Therefore, the Nusselt number of $Ti_3C_2$-Water-CMC 0.35wt% (0.083vol%) nanofluid is higher than $Ti_3C_2$-Water-CMC 0.7wt% (0.166vol%) nanofluid.

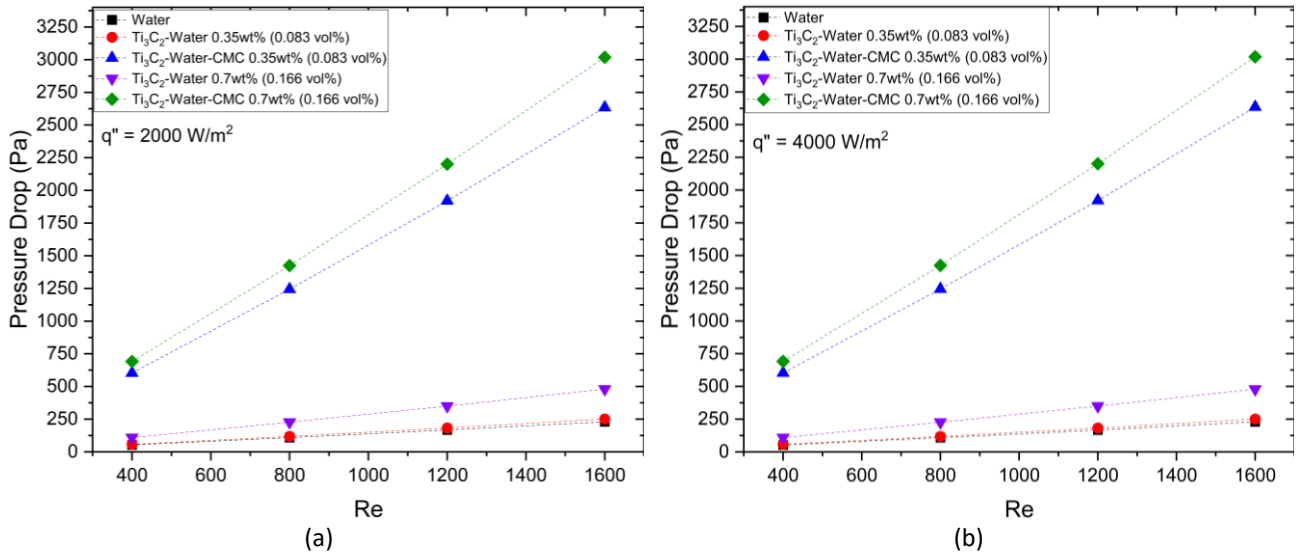


**Fig. 10.** Pressure Drop variation with Reynolds number for: (a) q" = 2000 W/m$^2$ (b) q" = 4000 W/m$^2$

Furthermore, Figure 10 shows the pressure drop as a function of the Reynolds number for different working fluids. The result shows that $Ti_3C_2$-Water-CMC 0.7wt% (0.166vol%) nanofluid has a significant increase in pressure drop of 1212.147% compared to Water at Reynolds numbers of 1600 for both 2000 W/m$^2$ and 4000 W/m$^2$ wall heat flux. Thus, the heat transfer performance and the pressure drop during fluid flow in the pipe must be considered for optimum results.

### *3.2 Optimum Heat Transfer*

Optimum heat transfer at the lowest pressure drop can be estimated using the Design Expert Optimization algorithm. The constraints of the present optimization can be seen in Table 3. Furthermore, the top 5 optimization results can be seen in Table 4.

The ramps' view of the optimization point can be found in Figure 11. Based on the multi-objective criteria observed in the research, $Ti_3C_2$-Water-CMC 0.35wt% (0.083vol%) nanofluid is the most optimum nanofluid chosen since it can satisfy the increasing heat transfer performance and a minimum increase in pressure drop. This nanofluid achieves the optimum performance in 1235.408 Reynolds numbers and 3999.95 W/m$^2$ heat flux, which results in 74.514 for the Nusselt number and 1998.739 Pa for the pressure drop.

**Table 3**
Optimization constraints

| Name | Goal | Lower Limit | Upper Limit | Lower Weight | Upper Weight | Importance |
|---|---|---|---|---|---|---|
| Factor 1 :Reynolds Number | is in range | 400 | 1600 | 1 | 1 | 3 |
| Factor 2:Wall Heat Flux | is in range | 2000 | 4000 | 1 | 1 | 3 |
| Factor 3: Fluid | is in range | Water | $Ti_3C_2$-Water-CMC0.7wt%(0.166vol%) | 1 | 1 | 3 |
| Response 1: Nu (average) | maximize | 32.399 | 83.493 | 1 | 1 | 5 |
| Response 2: Pressure Drop | minimize | 52.672 | 3018.28 | 1 | 1 | 2 |

**Table 4**
Optimization constraints

| No. | Re | Wall Heat Flux ($W/m^2$) | Fluid | Nu (average) | Pressure Drop (Pa) | Desirability | |
|---|---|---|---|---|---|---|---|
| 1 | 1235.408 | 3999.950 | $Ti_3C_2$-Water-CMC0.35wt%(0.083vol%) | 74.514 | 1998.739 | 0.642 | Selected |
| 2 | 1240.234 | 3998.366 | $Ti_3C_2$-Water-CMC0.35wt%(0.083vol%) | 74.649 | 2006.904 | 0.642 | |
| 3 | 1227.247 | 3999.409 | $Ti_3C_2$-Water-CMC0.35wt%(0.083vol%) | 74.286 | 1984.929 | 0.642 | |
| 4 | 1245.353 | 3999.839 | $Ti_3C_2$-Water-CMC0.35wt%(0.083vol%) | 74.792 | 2015.565 | 0.642 | |
| 5 | 1243.155 | 3983.383 | $Ti_3C_2$-Water-CMC0.35wt%(0.083vol%) | 74.728 | 2011.847 | 0.642 | |

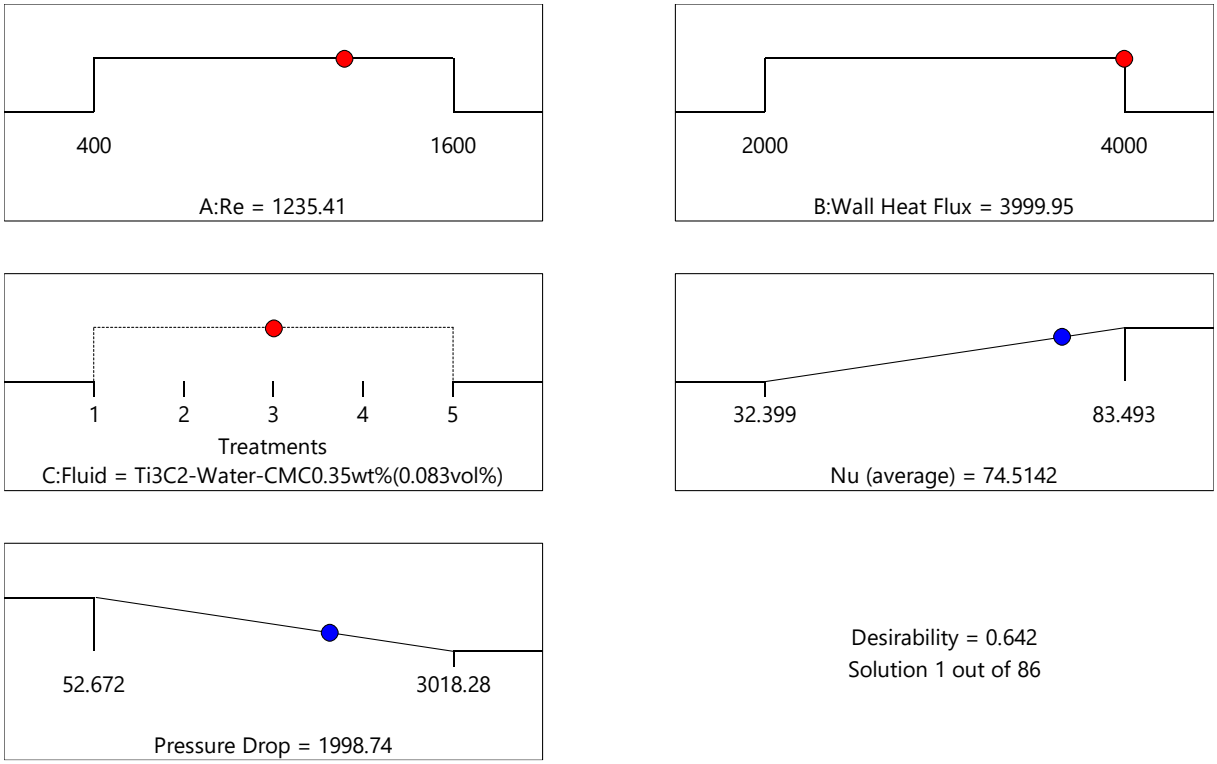


**Fig. 11.** Ramp's view of optimum point

## 4. Conclusions

MXene $Ti_3C_2$-Water and $Ti_3C_2$-Water-CMC were successfully evaluated using a numerical approach with the effective thermophysical properties method. The trade-off between heat transfer performance and pressure drop for the nanofluid was solved using Design Expert numerical optimization. The optimal $Ti_3C_2$ nanofluid that satisfies the increasing heat transfer performance and decreasing pressure drop is the $Ti_3C_2$-Water-CMC 0.35wt% (0.083vol%) nanofluid. This nanofluid achieves the optimum heat transfer performance at 1235.408 Reynolds number and 3999.95 W/m$^2$ heat flux, which results in 74.514 for Nusselt number and 1998.739 Pa for pressure drop.

## Acknowledgment

Financial support from the Directorate of Research and Development Universitas Indonesia through Riset Kolaborasi Indonesia 2023, NKB-1070/UN2.RST/HKP.05.00/2023 is truly acknowledged.

## References

[1] Choi, S. US and Jeffrey A. Eastman. *Enhancing thermal conductivity of fluids with nanoparticles*. No. ANL/MSD/CP-84938; CONF-951135-29. Argonne National Lab.(ANL), Argonne, IL (United States), 1995.

[2] Eastman, Jeffrey A., S. R. Phillpot, S. U. S. Choi and P. Keblinski. "Thermal transport in nanofluids." *Annu. Rev. Mater. Res.* 34, no. 1 (2004): 219-246. https://doi.org/10.1146/annurev.matsci.34.052803.090621

[3] Warrier, Pramod and Amyn Teja. "Effect of particle size on the thermal conductivity of nanofluids containing metallic nanoparticles." *Nanoscale research letters* 6 (2011): 1-6. https://doi.org/10.1186/1556-276X-6-247

[4] Hung, Tu-Chieh, Wei-Mon Yan, Xiao-Dong Wang and Chun-Yen Chang. "Heat transfer enhancement in microchannel heat sinks using nanofluids." *International Journal of Heat and Mass Transfer* 55, no. 9-10 (2012): 2559-2570. https://doi.org/10.1016/j.ijheatmasstransfer.2012.01.004

[5] Mohammed, H. A., P. Gunnasegaran and N. H. Shuaib. "Heat transfer in rectangular microchannels heat sink using nanofluids." *International Communications in Heat and Mass Transfer* 37, no. 10 (2010): 1496-1503. https://doi.org/10.1016/j.icheatmasstransfer.2010.08.020

[6] Lee, Ji-Hwan, Seung-Hyun Lee and Seok Pil Jang. "Do temperature and nanoparticle size affect the thermal conductivity of alumina nanofluids?." *Applied Physics Letters* 104, no. 16 (2014). https://doi.org/10.1063/1.4872164

[7] Kim, Sang Hyun, Sun Rock Choi and Dongsik Kim. "Thermal conductivity of metal-oxide nanofluids: particle size dependence and effect of laser irradiation." (2007): 298-307. https://doi.org/10.1115/1.2427071

[8] Naguib, Michael, Michel W. Barsoum and Yury Gogotsi. "Ten years of progress in the synthesis and development of MXenes." *Advanced Materials* 33, no. 39 (2021): 2103393. https://doi.org/10.1002/adma.202103393

[9] Mao, Mingyang, Ding Lou, Danling Wang, Hammad Younes, Haiping Hong, Hang Chen and G. P. Peterson. "Ti3C2Tx MXene nanofluids with enhanced thermal conductivity." *Chemical Thermodynamics and Thermal Analysis* 8 (2022): 100077. https://doi.org/10.1016/j.ctta.2022.100077

[10] Ma, Xin, Liu Yang, Guoying Xu and Jianzhong Song. "A comprehensive review of MXene-based nanofluids: preparation, stability, physical properties and applications." *Journal of Molecular Liquids* 365 (2022): 120037. https://doi.org/10.1016/j.molliq.2022.120037

[11] Ambreen, Tehmina, Arslan Saleem and Cheol Woo Park. "Thermal efficiency of eco-friendly MXene based nanofluid for performance enhancement of a pin-fin heat sink: Experimental and numerical analyses." *International Journal of Heat and Mass Transfer* 186 (2022): 122451. https://doi.org/10.1016/j.ijheatmasstransfer.2021.122451

[12] Aslfattahi, Navid, L. Samylingam, A. S. Abdelrazik, A. Arifutzzaman and R. J. S. E. M. Saidur. "MXene based new class of silicone oil nanofluids for the performance improvement of concentrated photovoltaic thermal collector." *Solar Energy Materials and Solar Cells* 211 (2020): 110526. https://doi.org/10.1016/j.solmat.2020.110526

[13] Samylingam, L., Navid Aslfattahi, R. Saidur, Syed Mohd Yahya, Asif Afzal, A. Arifutzzaman, K. H. Tan and K. Kadirgama. "Thermal and energy performance improvement of hybrid PV/T system by using olein palm oil with MXene as a new class of heat transfer fluid." *Solar Energy Materials and Solar Cells* 218 (2020): 110754. https://doi.org/10.1016/j.solmat.2020.110754

[14] Rahmadiawan, Dieter, Shih Chen Shi, Zahrul Fuadi, Hairul Abral, Nandy Putra, Ridho Irwansyah, Dedison Gasni and Andhy M. Fathoni. "Experimental investigation on stability, tribological, viscosity and thermal conductivity of MXene/Carboxymethyl cellulose (CMC) water-based nanofluid lubricant." *J. Tribol* 39 (2023): 36-50.

[15] Minea, Alina Adriana, Bernardo Buonomo, Jonas Burggraf, Davide Ercole, Kavien Raaj Karpaiya, Anna Di Pasqua, Ghofrane Sekrani *et al.,* "NanoRound: A benchmark study on the numerical approach in nanofluids' simulation." *International Communications in Heat and Mass Transfer* 108 (2019): 104292. https://doi.org/10.1016/j.icheatmasstransfer.2019.104292

[16] Dehghan, Peymaneh, Fatemeh Keramat, Masoud Mofarahi and Chang-Ha Lee. "Computational fluid dynamic analysis of graphene oxide/water nanofluid heat transfer over a double backward-facing microchannel." *Journal of the Taiwan Institute of Chemical Engineers* 145 (2023): 104821. https://doi.org/10.1016/j.jtice.2023.104821

[17] Elfaghi, Abdulhafid MA, Alhadi A. Abosbaia, Munir FA Alkbir and Abdoulhdi AB Omran. "Heat transfer enhancement in pipe using Al2O3/water nanofluid." *CFD Letters* 14, no. 9 (2022): 118-124. https://doi.org/10.37934/cfdl.14.9.118124

[18] Cengel, Yunus and John Cimbala. *Ebook: Fluid mechanics fundamentals and applications (si units)*. McGraw Hill, 2013.

[19] Bennia, A. and M. N. Bouaziz. "CFD modeling of turbulent forced convective heat transfer and friction factor in a tube for Fe3O4 magnetic nanofluid in the presence of a magnetic field." *Journal of the Taiwan Institute of Chemical Engineers* 78 (2017): 127-136. https://doi.org/10.1016/j.jtice.2017.04.035

[20] Wen, Dongsheng and Yulong Ding. "Experimental investigation into convective heat transfer of nanofluids at the entrance region under laminar flow conditions." *International journal of heat and mass transfer* 47, no. 24 (2004): 5181-5188. https://doi.org/10.1016/j.ijheatmasstransfer.2004.07.012

[21] Xuan, Yimin and Wilfried Roetzel. "Conceptions for heat transfer correlation of nanofluids." *International Journal of heat and Mass transfer* 43, no. 19 (2000): 3701-3707. https://doi.org/10.1016/S0017-9310(99)00369-5